Environment Protection Engineering

Vol. 44 2018 No. 3

DOI: 10.5277/epe180304

ADRIANA SALDAÑA-ROBLES[1], ALBERTO SALDAÑA-ROBLES[1], ALFREDO MÁRQUEZ-HERRERA[1], GRACIELA MA DE LA LUZ RUIZ-AGUILAR[1], ADRIÁN FLORES-ORTEGA[1], NOÉ SALDAÑA-ROBLES[1]

ADSORPTION OF ARSENIC ON GRANULAR FERRIC HYDROXIDE (GEH®). IMPACT OF INITIAL CONCENTRATION OF ARSENIC(V) ON KINETICS AND EQUILIBRIUM STATE

The present study discusses the adsorption kinetics of arsenic(V) on granular ferric hydroxide (GEH) and the GEH adsorption capacity for arsenic(V) at equilibrium. The impact of temperature on GEH adsorption capacity was studied, as well as the effects of the initial concentration of arsenic(V) and GEH concentration on the adsorption rates of arsenic(V). The Freundlich isotherm describes the arsenic(V) adsorption behavior reasonably well ($r^2 > 0.965$). The adsorption kinetics was studied by fitting the experimental data to both first-order and second-order models. The maximum adsorption capacity of arsenic(V) on GEH was 2.701 $mg \cdot g^{-1}$, which is higher than the adsorption capacities of other adsorbents reported. The kinetics of arsenic(V) adsorption was well defined by the second-order model, with the correlation coefficients in the range of 0.960–0.987. This study shows that due to its properties, GEH is a good candidate for removal of arsenic(V) from groundwater.

1. INTRODUCTION

The presence of arsenic (As) in groundwater, which may be due to natural contamination, is a problem that affects several areas around the world that have relatively higher arsenic concentrations than the guidelines published by the World Health Organization (WHO). These areas include Bangladesh, Spain, Nicaragua, Peru, Argentina, Mexico, and Chile, among others [1]. In Mexico, water from mine drainage systems contains up to 7 $mg \cdot dm^{-3}$ of arsenic [2, 3].

[1]División Ciencias de la Vida, Campus Salamanca-Irapuato, Universidad de Guanajuato, Ex Hacienda El Copal, Km. 9 Carretera Irapuato-Silao, Irapuato, GTO, corresponding author N. Saldaña-Robles, e-mail address: ssalrrob@gmail.com

The principal source of dissolved arsenic in groundwater is often the mobilization of natural deposits in rocks, sediments, and soils. Another important source of arsenic in groundwater is the reductive dissolution of arsenic-bearing iron and other oxyhydroxides [4]. Industrial waste discharges containing arsenic are an important anthropogenic contribution to pollution in some regions of Chile and Mexico. The presence of arsenic in water represents a risk for human health [5]. Arsenic causes serious health problems, such as cancers and skin diseases, among others. These ailments have been linked to arsenic ingestion [6–8].

Due to the high toxicity of arsenic, the WHO has changed the guideline value for arsenic in drinking water from 0.05 to 0.01 $mg \cdot dm^{-3}$ [9], and the U.S. Health Ministry (SAA) of Mexico has implemented a new maximum contaminant level for arsenic in drinking water at 0.025 $mg \cdot dm^{-3}$ [10]. These arsenic standards will lead to change in infrastructure to upgrade existing water treatment systems and develop new treatment options [11].

The most popular techniques used for removing arsenic(V) from aqueous matrixes are as follows: adsorption/precipitation: mainly processes on oxides/hydroxides, iron, activated carbon and activated alumina; coagulation/precipitation: processes using metal salts of elements such as aluminum or iron, ion-exchange, and desalting techniques such as reverse osmosis. Reverse osmosis is expensive, however, it is capable of decreasing arsenic(V) concentrations below 0.01 $mg \cdot dm^{-3}$. This process typically removes arsenic(V) at 98–99% [12–14].

Properties of several adsorbents have been studied towards the adsorption of arsenic from groundwater. A variety of different materials are widely used due to their good sorption properties; these include iron hydroxides, which are present in various materials such as granular ferric hydroxide, zero-valent iron, and iron minerals such as magnetite and goethite [15–19].

However, little has been done to determine the impact of initial arsenic concentration on its adsorption on GEH to receive product water suitable for irrigation purpose. The aim of this study is to understand the impact of the initial concentration of arsenic(V) and GEH concentration on the arsenic removal kinetics and adsorption capacities for irrigation conditions required in Guanajuato, Mexico.

2. MATERIALS AND METHODS

Adsorbent. Commercial granular ferric hydroxide, GEH (GEH Wasserchemie GmbH, Germany) was the adsorbent used in this study. The adsorbent was characterized by X-ray and by scanning electron microscopy (SEM). The particle size of the GEH used was in the range of 0.5–1.0 mm. This adsorbent has a large specific surface area and high porosity. The characteristics and properties of GEH reported in the literature are given in Table 1.

Table 1

Properties of GEH [20]

Parameter	Value
Bulk density	1.22–1.29 g·dm^{-3} wet
Porosity	72–77%
Surface area	250–300 m^2·g^{-1}
Moisture content	43–48%
Components	β-FeOOH and Fe(OH)^3
pH_{ZPC}	7.6–7.8
Grain size	0.32–2 mm

Reagents. Arsenate solutions were prepared from reagent grade $Na_2HAsO_4 \cdot 7H_2O$ (Sigma-Aldrich, Mexico) dissolved in distilled water. All chemicals used were laboratory reagent grade (99.98% pure).

Adsorption isotherms. Different quantities of GEH ranging from 0 to 0.705 g·dm^{-3} (Table 2) were placed in 500 cm^3 flasks containing 0.800 mg·dm^{-3} arsenic(V) in solution, and pH adjusted to 7.4. The flasks were stirred at 220 rpm using a New Brunswick Scientific shaker for 24 h, at three temperatures (12, 25, and 45 °C). Each data set included a blank control sample (without GEH). pH of each sample was adjusted using a stock solution of either HNO_3 or NaOH. The sample bulk volume was modified by approximately 0.75% by the addition of stock solutions. The samples were collected after 24 h, filtered and analyzed for arsenic by the molybdenum blue method [21].

Table 2

Quantitied of GEH used at various temperatures [g/dm^3]

Sample	Temperature [°C]			Sample	Temperature [°C]		
	12	25	45		12	25	45
1	0.000	0.000	0.000	8	0.250	0.253	0.252
2	0.010	0.011	0.011	9	0.325	0.323	0.323
3	0.021	0.023	0.022	10	0.451	0.453	0.451
4	0.028	0.028	0.027	11	0.526	0.528	0.527
5	0.078	0.077	0.078	12	0.626	0.627	0.624
6	0.138	0.136	0.136	13	0.700	0.705	0.703
7	0.200	0.202	0.202				

The Freundlich model was used to estimate the maximum adsorption capacity of GEH for arsenic(V). The mathematical expression of the Freundlich isotherm is given by

$$q_e = K_F C_e^{1/n} \tag{1}$$

where C_e (mg·dm^{-3}) is the pseudo-equilibrium concentration, q_e (mg·g^{-1}) is the amount of adsorbed arsenic at pseudo-equilibrium, K_F (mg·g^{-1}) is a measure of the adsorption capacity, and $1/n$ is considered a measure of surface heterogeneity and surface affinity for the solute.

Adsorption kinetics. Experiments of arsenic adsorption kinetic were conducted at 25 °C and pH 7.4 in a system consisting of a 5 dm^3 reactor stirrer at 220 rpm. Three quantities of GEH (0.357, 1.000, and 2.000 g·dm^{-3}) and two initial concentrations of arsenic(V) (0.450 and 0.800 mg·dm^{-3}) were used. The samples were collected at different time intervals over the course of 12 h. A previous study revealed that most arsenic is removed within the first 6 h [5]. Each set of samples was filtered using a 0.45 μm cellulose nitrate membrane filter. pH was adjusted initially and during the experiment to reach the desired condition using a stock solution of either HNO_3 or NaOH. The sample bulk volume was modified by approximately 0.05% upon addition of the stock solutions. To evaluate the kinetic order of the adsorption process, first order and second order models were applied. The kinetic models were tested by a least-square regression analysis to determine which equation best described the data set.

3. RESULTS AND DISCUSSION

3.1. GEH CHARACTERISTICS

Elemental chemical analysis by X-ray diffraction showed an amorphous iron mineral without defined crystalline structure with more than two oxygen atoms per iron atom (Table 3).

Table 3

Results of X-ray diffraction analysis of GEH

Element	Weight %	% of atoms
Fe content	58.71	29.20
O content	36.90	64.06
Cl content	2.02	1.58
C content	2.14	4.96
S content	0.23	0.20
Mn content	0.000017	0.000017
O/Fe ratio	0.63	2.19
Fe/S ratio	255.3	146
Particle density, g/cm^3	1.67	

The surface morphology of GEH was determined by SEM. The images captured are shown in Fig. 1.

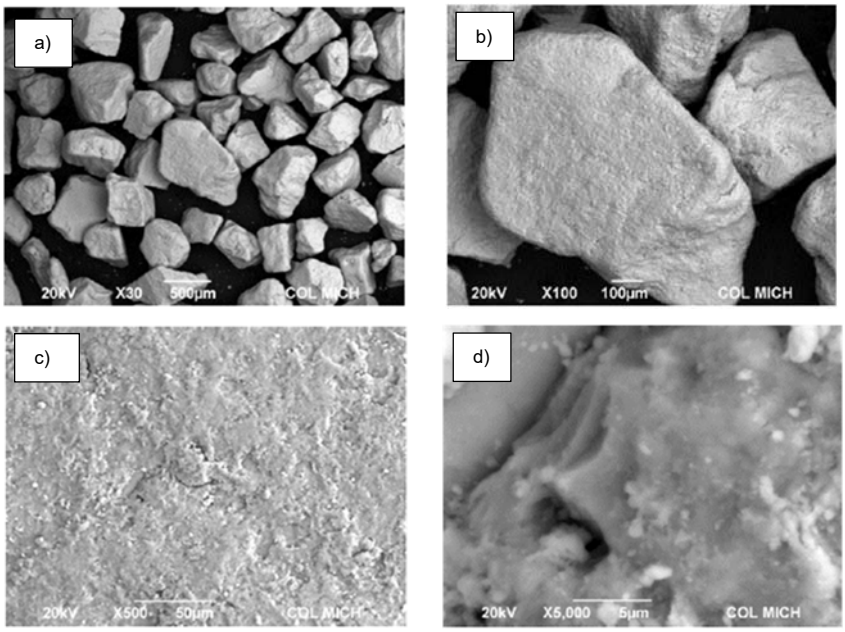

Fig. 1. SEM images of GEH at the magnification of: a) 30×, b) 100×, c) 500×, d) 5000×

These SEM images show that the GEH grains have an irregular and smooth shape, a large size and rough surface.

3.2. ADSORPTION ISOTHERMS

The parameters of the adsorption isotherms for arsenic(V) at 12, 25, and 45 °C at pH 7.4 are given in Table 4. The high correlation coefficient ($r^2 > 0.96$) suggests that the experimental data fit the Freundlich model reasonably well.

Table 4

Freundlich isotherm parameters
for arsenic(V) at pH 7.4

Temperature [°C]	K_F [mg·g^{-1}]	1/n	r^2
12	2.241	0.239	0.965
25	2.589	0.221	0.967
45	2.701	0.142	0.976

The adsorption capacity (K_F) increases when the temperature increases. It is a signal of an endothermic adsorption, as previously reported [5]. The endothermic adsorption

implies either a greater amount of arsenic retained by the GEH, which is related to an increase in the number of sites available for adsorption or a reduction in the mass transfer resistance of the arsenic in the boundary layer near to the GEH. The latter case could be favored by the fact that at elevated temperatures endothermic transport mechanisms such as diffusion become more important, and thus facilitate the motion of arsenic onto the GEH. On the other hand, the 1/*n* values indicate a favorable adsorption of arsenic(V) on GEH (the degree of sorption increases as 1/*n* approaches zero [5]). Figure 2 clearly shows the influence of temperature on adsorption isotherms for arsenic(V) at pH 7.4.

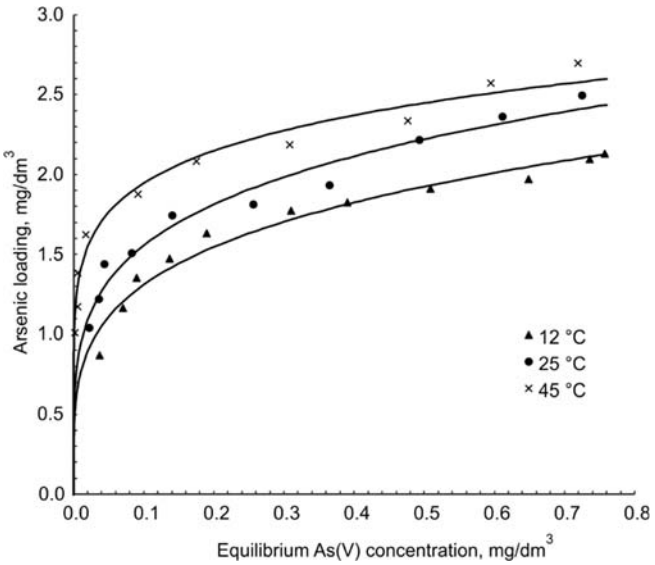

Fig. 2. Adsorption isotherms for arsenic(V) at pH 7.4

Table 5 shows a comparison among several adsorbents found in other isotherm studies for arsenic(V), such as carbon modified with iron nanoparticles (CFe), and iron carbide from the pyrolyzed crown leaves of pineapple (CarFe). For these materials, the adsorption capacities were 0.990 and 1.40 mg·g^{-1}, respectively [22]. Aluminum doped nano manganese copper ferric has an adsorption capacity of 0.853 mg·g^{-1} [23]. Other authors reported test results of arsenic(V) adsorption on multi-walled boron-nitride nanotubes (BNNT) that show an adsorption capacity of 1.969 mg·g^{-1} [6]. For nano aluminium doped manganese copper ferrite polymer (NADMCF) [23], BNNT [6], kaolinite [24], GAC-Fe [25], and akageneite nanostructures [26], the adsorption is compatible with a multilayer adsorption. Adsorption of arsenic onto CFe, CarFe, NADMCF and BNNT adsorbents describes well the Freundlich model with adsorption capacity ranging from 0.99 to 2.59 mg·g^{-1}. Kaolinite, GAC-Fe, GAC-Fe-O_2, and akageneite nanostructures present a predominantly monolayer adsorption with an adsorption capacity ranging from 0.008 to 2.96 mg·g^{-1}. In this work, the adsorption capacity of GEH was found

to be 2.589 $mg \cdot g^{-1}$ (at 25 °C). Thus, we observed that the GEH has a good adsorption capacity in comparison with other adsorbents found in the literature.

Table 5

Sorption capacities of various adsorbents towards arsenic(V)

Adsorbent	Capacity [$mg \cdot g^{-1}$]	Model used	Temperature [°C]	pH	Reference
CFe	0.99	Freundlich	25	7.0	[22]
CarFe	1.44			7.0	
NADMCF	0.85			6.0	[23]
BNNT	1.97			6.9	[6]
Kaolinite	<0.23	Langmuir		5.5	[24]
Untreated GAC	0.038			4.7	[25]
GAC-Fe (0.05 M)	2.96			4.7	
GAC-Fe-O_2 (0.05 M)	1.92			4.7	
Akaganeite nanostructures	1.80			7.5	[26]
GEH	3.13	Freundlich	20	6.5	[5]
GEH	4.08		30	6.5	
GEH	4.57		40	6.5	
GEH, grain size 0.15–0.18 mm	3.6		24	7.0	[27]
GEH, grain size 0.2–0.4 mm	3.5			7.0	[28]
GEH	3.67		25	7.0	[29]
GEH, grain size 0.5–1.0 mm	2.59			7.4	present work

This study considers pH and As concentration ranges, which are similar to real conditions found in water used for irrigation in the region of Guanajuato, Mexico. Whereas, drinking water of the region presented As concentration ranges from 0.01 to 0.03 $mg \cdot dm^{-3}$, groundwater used for irrigation in Irapuato, Guanajuato, presented an As concentration of 0.33 $mg \cdot dm^{-3}$ [30]. Thus, the adsorption capacity of arsenic(V) onto GEH found in the present work may be considered as a well approximation to the actual working conditions in Guanajuato. Other researchers focused on drinking water under several conditions of pH and grain sizes of GEH that provides greater adsorption capacities of arsenic onto GEH than the present work, however we argue that these conditions are not practical for the irrigation requirements of the studied region of Guanajuato, Mexico.

3.3. ARSENIC(V) REMOVAL KINETIC STUDIES

The arsenic(V) removal time dependences at various quantities of GEH and for both concentrations of arsenic(0.450 $mg \cdot dm^{-3}$ and 0.800 $mg \cdot dm^{-3}$) are shown in Figs. 3a, b, respectively. These results indicated a rapid initial uptake of arsenic(V), followed by a slower removal, which finally approaches a plateau. The results showed that a higher

quantity of GEH increases the uptake rate of arsenic(V). In the first 60 min, approximately 90–92% of arsenic was removed for concentrations of 1 and 2 g·dm^{-3} GEH. For 0.357 g·dm^{-3} GEH, arsenic removal was approximately 40–45% within the first 60 min. The slow arsenic adsorption on GEH observed after the first 60 min can be explained by the low concentration gradient between the solution and the adsorbent surface, which diminishes the arsenic transport between the two phases. When the adsorption/desorption approached equilibrium, approximately 98–99% of arsenic(V) was adsorbed for 1 and 2 g·dm^{-3} GEH, while at 0.357 g·dm^{-3} GEH, only 62–69% of arsenic was adsorbed; this behavior was observed for both concentrations of arsenic.

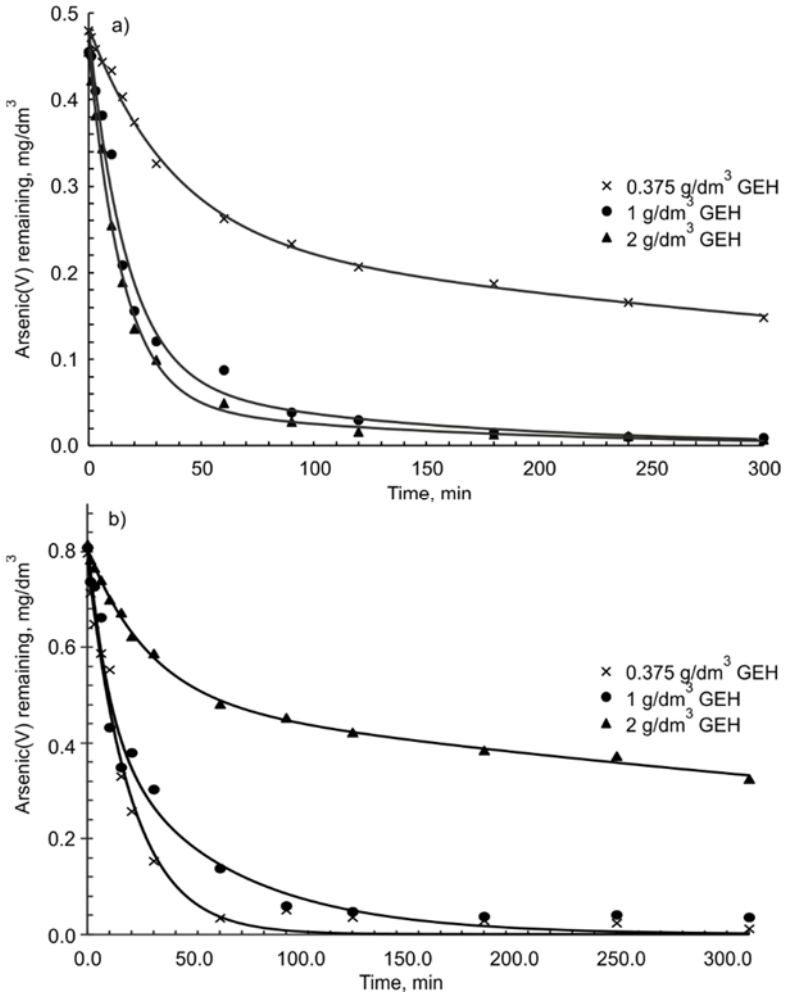

Fig. 3. Adsorption kinetics for arsenic(V) at the concentrations of:
a) 0.450 mg·dm^{-3}, b) 0.800 mg·dm^{-3}

To evaluate the model order of the adsorption process, first and second order kinetic models were analyzed. The first order models imply that the adsorption rate is proportional to the concentration gradient, whereas the second order models imply that the reaction rate is proportional to the square of the concentration gradient. The lineal transformation of both order type of kinetic models are given by:

- First order

$$\ln[\mathrm{As}]_t = \ln [\mathrm{As}]_0 - k_1 t \tag{2}$$

- Second order

$$\frac{1}{[\mathrm{As}]_t} - \frac{1}{[\mathrm{As}]_0} = k_2 t \tag{3}$$

where k_1 and k_2 are the reaction rate constants for the first and second order respectively, $[\mathrm{As}]_t$ is the arsenic concentration at a time t and $[\mathrm{As}]_0$ is the initial arsenic concentration ($t = 0$).

Table 6

Pearson coefficient (r^2), standard error (SE) and rate constants (k) for the kinetic model tested

Arsenic(V) concentration [mg·dm^{-3}]	GEH [g·dm^{-3}]	Kinetic model				
		First order $\ln([\mathrm{As}]_t/[\mathrm{As}]_0)$ vs. t		Second order $1/[\mathrm{As}]_t - 1/[\mathrm{As}]_0$ vs. t		
		SE	r^2	SE	r^2	k [mg^{-1}·dm^3·min^{-1}]
0.450	0.36	0.044	0.889	0.027	0.960	0.017
	1.00	0.085	0.897	0.080	0.981	0.355
	2.00	0.102	0.844	0.062	0.980	0.418
0.800	0.36	0.226	0.901	0.061	0.960	0.007
	1.00	0.178	0.838	0.066	0.978	0.116
	2.00	0.170	0.840	0.118	0.987	0.237

The correlation coefficient (r^2) and the standard error (SE) were calculated for each kinetic model given by Eqs. (2) and (3). Their values are given in Table 6. The SE values for the second order kinetic model are lower than those for the first order kinetic model; this suggests that the second order kinetic model generally best describes the experimental data for all quantities of GEH and for both concentrations of arsenic(V) tested.

Since the second order model better describes the parameters, Table 6 shows the second order rate constants (k) for all quantities of GEH tested at both concentrations of arsenic. The correlation coefficients (r^2) ranged between 0.96–0.99, while the values of k ranged between 0.007 and 0.418 mg^{-1}·dm^3·min^{-1}. The value of k increased as the

amount of GEH increased. The rate constant increases as the amount of GEH increases. As more GEH is introduced in the solution, more adsorption sites are available. Consequently, the rate constant is increased.

4. CONCLUSIONS

The Freundlich model describes the adsorption isotherm of arsenic(V) reasonably well, indicating that the surface of the adsorbent is heterogeneous. The adsorption capacity increases upon increasing temperature. The kinetic adsorption rate of arsenic(V) is highest at the first 90 min. Approximately 95% of the arsenic(V) was adsorbed during this period. This behavior was observed for both concentrations of arsenic. Approximately 45–50% of arsenic(V) was removed by 0.357 $g \cdot dm^{-3}$ GEH within the first 90 min, this behavior was observed for both concentrations of arsenic. The measured adsorption rate data were well fitted by a second order kinetic model. The amount of adsorbent influences the adsorption kinetics of arsenic(V). The rate of adsorption of arsenic(V) increases as GEH contents increases.

These results showed that the GEH is one of the better adsorbents in comparison with the adsorbents reported in the literature.

Finally, the adsorption capacity depends on pH, temperature, and grain size of the GEH. The adsorption capacity increases as pH and grain size decreases, and temperature increases. The latter points to endothermic process of adsorption, which could be related either to an increase of active sites available for adsorption upon increasing temperature or to reduction in the mass transfer resistance of the arsenic in the boundary layer near to the GEH.

ACKNOWLEDGEMENT

The authors would like to thank CIATEC for its financial support (GD 0065 project).

REFERENCES

[1] KOLBE F., WEISS H., MORGENSTERN P., WENNRICH R., LORENZ W., SCHURK K., STANJEK H., DAUS B., *Sorption of aqueous antimony and arsenic species onto akaganeite*, J. Colloid Interface Sci., 2011, 357 (2), 460.

[2] RAZO I., CARRIZALES L., CASTRO J., DÍAZ-BARRIGA F., MONROY M., *Arsenic and heavy metal pollution of soil, water and sediments in a semi-arid climate mining area in Mexico*, Water Air Soil Pollut., 2004, 154 (1), 129.

[3] SONG S., LOPEZ A., HERNANDEZ D.J., PENG C., MONROY-FERNANDEZ M.G., RAZO-SOTO I., *Arsenic removal from high-arsenic water by enhanced coagulation with ferric ions and coarse calcite*, Water Res. J., 2006, 40 (2), 364.

[4] CAMACHO L.M., GUTIÉRREZ M., ALARCÓN M.T., VILLALBA M.L., DENG S., *Occurrence and treatment of arsenic in groundwater and soil in northern Mexico and southwestern USA*, Chemosphere, 2011, 83 (3), 211.

[5] BANERJEE K., GARY L.A., PREVOST M., NOUR S., JEKEL M., GALLAGHER P.M., BLUMENSCHEIN C.D., *Kinetic and thermodynamic aspects of adsorption of arsenic onto granular ferric hydroxide (GFH)*, Water Res., 2008, 42, 3371.
[6] CHEN R., ZHI C., YANG H., BANDO Y., ZHANG Z., SUGIUR N., GOLBERG D., *Arsenic(V) adsorption on Fe_3O_4 nanoparticle-coated boron nitride nanotubes*, J. Colloid Interface Sci., 2011, 359 (1), 261.
[7] LAMM S.H., ROBBINS S.A., ZHOU C., LU J., CHEN R., FEINLEIB M., *Bladder/lung cancer mortality in blackfoot-disease (BFD). Endemic area villages with low (<150 μg/L) well water arsenic levels. An exploration of the dose–response Poisson analysis*, Regul. Toxicol. Pharmacol., 2013, 65, 147.
[8] LIN H.J., SUNG T.I., CHEN C.Y., GUO H.R., *Arsenic levels in drinking water and mortality of liver cancer in Taiwan,* J. Hazard. Mater., 2013, 262, 1132.
[9] WHO, *Guidelines for Drinking Water Quality*, *1. Recommendations*, World Health Organization, Geneva 1993.
[10] Mexican Official Norm, NOM-127-SSA-1994, 2000. *Environmental health, water for use and human intake – permissible limits of quality and treatments that must be applied for water purification.*
[11] BASKAN M.B., PALA A., *Removal of arsenic from drinking water using modified natural zeolite,* Desalination, 2011, 281, 396.
[12] MOSTAFA M.G., CHEN Y.H., JEAN J.S., *Kinetics and mechanism of arsenate removal by nanosized iron oxide-coated perlite*, J. Hazard. Mater., 2011, 187, 89.
[13] GILES D.E., MOHAPATRA M., ISSA T.B., *Iron and aluminum based adsorption strategies for removing arsenic from water,* J. Environ. Manage., 2011, 92, 3011.
[14] JAIN C.K., SINGH R.D., *Technological options for the removal of arsenic with special reference to South East Asia*, J. Environ. Manage., 2012, 107, 1.
[15] AREDES S., KLEIN B., PAWLIK M., *The removal of arsenic from water using natural iron oxide minerals*, J. Clean Prod., 2012, 29–30, 208.
[16] NIETO C., RANGEL J.R., *Anchorage of iron hydro(oxide) nanoparticles onto activated carbon to remove As(V) from water*, Water Res., 2012, 46 (9), 2973.
[17] TRESINTSI S., SIMEONIDIS K., VOURLIAS G., STAVROPOULOS G., MITRAKAS M., *Kilogram-scale synthesis of iron oxyhydroxides with improved arsenic removal capacity. Study of Fe(II) oxidation/precipitation parameters*, Water Res., 2012, 46 (16), 5255.
[18] TANBOONCHUY V., GRISDANURAK G., LIAO C.H., *Background species effect on aqueous arsenic removal by nano zero-valent iron using fractional factorial design*, J. Environ. Manage., 2012, 205–206, 40.
[19] JIANG W., CHEN X., NIU Y., PAN B., *Spherical polystyrene-supported nano-Fe_3O_4 of high capacity and low-field separation for arsenate removal from water*, J. Hazard. Mater., 2012, 243, 319.
[20] DRIEHAUS W., *Arsenic removal from drinking water. The GEH® process*, AWWA Inorganic Contaminants Workshop, Albuquerque, NM, U.S.A., 2000.
[21] HU S., LU J., JING C., *A novel colorimetric method for field arsenic speciation analysis*, J. Environ. Sci., 2012, 24 (7), 1341.
[22] GUTIÉRREZ O.E., GARCÍA G., ORDOÑEZ E., OLGUÍN M.T., CABRAL-PRIETO A., *Synthesis, characterization and adsorptive properties of carbon with iron nanoparticles and iron carbide for the removal of As(V) from water*, J. Environ. Manage., 2013, 114, 1.
[23] MALANA M.A., QURESHI R.B., ASHIQ M.N., *Adsorption studies of arsenic on nano aluminium doped manganese copper ferrite polymer (MA, VA, AA) composite: Kinetics and mechanism*, Chem. Eng. J., 2011, 172 (2–3), 721.
[24] LADEIRA A.C.Q., CIMINELLI V.S.T., *Adsorption and desorption of arsenic on an oxisol and its constituents*, Water Res., 2004, 38 (8), 2087.
[25] GU Z., FANG J., DENG B., *Preparation and evaluation of GAC-based iron-containing adsorbents for arsenic removal*, Environ. Sci. Technol., 2005, 39 (10), 3833.

[26] DELIYANNI E.A., BAKOYANNAKIS D.N., ZOUBOULIS A.I., MATIS K.A., *Sorption of As(V) ions by alaganeite-type nanocrystals*, Chemosphere, 2003, 50 (1), 155.
[27] BADRUZZAMAN M., WESTERHOFF P., KNAPPE D.R.U., *Intraparticle diffusion and adsorption of arsenate onto granular ferric hydroxide (GFH)*, Water Res., 2004, 38, 4002.
[28] AMY G., CHEN, H., BRANDHUBER N., GRAZIANO N., VON GUNTEN U., CHOWDHURY Z., KOMMINENI S., BANERJEE K., JEKEL M., *Impact of water quality parameters on adsorbent treatment technologies for arsenic removal*, AWWA Research Foundation, 2004.
[29] HIGHFIELD D.E., *Arsenic occurrence in metro Phoenix ground water and treatment by granular ferric hydroxide*, MS Thesis, Arizona State University, Tempe 2002.
[30] RODRÍGUEZ R., MORALES-ARREDONDO I., RODRÍGUEZ I., *Geological differentiation of groundwater threshold concentrations of arsenic, vanadium and fluorine in El Bajio Guanajuatense, Mexico*, Geofísica Internacional, 2016, 55 (1), 5.